Manuscript Details

Manuscript number	MOLLIQ_2018_2388_R1
Title	Solvation structure for Fe(II), Co(II) and Ni(II) complexes in [P2225][NTf2] ionic liquids investigated by Raman spectroscopy and DFT calculation
Article type	Full length article

Abstract

The solvation structures of divalent iron, cobalt and nickel complexes in the ionic liquid, triethyl-n-pentylphosphonium bis(trifluoromethyl sulfonyl) amide ([P2225][NTf2]) were investigated by Raman spectroscopy. Based on a conventional analysis, the solvation numbers of Fe(II), Co(II), and Ni(II) in [P2225][NTf2] were determined to be 3.18, 3.21, and 3.14 at 298 K and 3.24, 3.32, and 3.37 at 373 K, respectively. From the temperature dependence of the Raman bands the isomerism of [NTf2]− from trans- to cis-coordinated isomer in the bulk and the first solvation sphere of the central M^{2+} (M=Fe, Co, and Ni) cation in [P2225][NTf2], thermodynamic properties such as $\Delta isoG$, $\Delta isoH$, and $\Delta isoS$ for the isomerism were evaluated. It was revealed that cis-[NTf2]− isomers were stabilized by enthalpic contribution, because $\Delta isoH(M)$ became remarkably negative in the first solvation sphere of the M^{2+} cation. Moreover, $\Delta isoH(M)$ contributed to the remarkable decrease in $\Delta isoG(M)$, and this result clearly indicates that cis-[NTf2]− conformers bound to M^{2+} cations are the preferred coordination state of [M(II)(cis NTf2)3]− in [P2225][NTf2]. The optimized geometries and the binding energies of [Fe(II)(cis-NTf2)3]−, [Co(II)(cis-NTf2)3]−, and [Ni(II)(cis-NTf2)3]− clusters were calculated by ADF simulations. The bonding energy, ΔEb, was calculated as $\Delta Eb = Etot(cluster) - Etot(M2+) - nEtot([NTf2]-)$, and ΔEb ([Fe(II)(cis-NTf2)3]−), $\Delta Eb([Co(II)(cis-NTf2)3]-)$, and $\Delta Eb([Ni(II)(cis-NTf2)3]-)$ were calculated to be −2132.1±6.4, −2254.6±6.1, and −2283.4±7.2 kJ mol−1, respectively. Furthermore, the bond distances of these clusters were consistent with the thermodynamic properties.

Keywords	Coordination state, DFT calculation, Iron group metal, Raman spectroscopy, Thermodynamic property
Manuscript category	Ionic liquids
Corresponding Author	Masahiko Matsumiya
Corresponding Author's Institution	Yokohama National University
Order of Authors	Yusuke Tsuchida, Masahiko Matsumiya, Katsuhiko Tsunashima
Suggested reviewers	Shridhar Gejji, Wesley A. Henderson, Patrik Johansson

Submission Files Included in this PDF

File Name [File Type]

cover_r.docx [Cover Letter]

reviewer.docx [Response to Reviewers]

Highlights_r.docx [Highlights]

manuscript_r.docx [Manuscript File]

Fig_r.docx [Figure]

Table_r.docx [Table]

To view all the submission files, including those not included in the PDF, click on the manuscript title on your EVISE Homepage, then click 'Download zip file'.

Research Data Related to this Submission

There are no linked research data sets for this submission. The following reason is given:
No data was used for the research described in the article

Dear Prof. W. Schröer

Editor-in-Chief of Journal of Molecular Liquids

Thank you for sending e-mail and many valuable reviewer comments.

The comments for each reviewer about the revised manuscript were written as follows.

We hope that the revised manuscript will be suitable for the publication.

Sincerely yours.

Dr. Masahiko Matsumiya,

Graduate School of Environment and Information Sciences,

Yokohama National University

E-mail/matsumiya-masahiko-dh@ynu.ac.jp

For Reviewer#1

Thank you for sending many useful comments.

According to your comments, the revised manuscript was corrected as follows.

A nice manuscript very appropriate to the journal.

Mandatory: My only query concerns to the Conclusions style. Please, Conclusions are not a summary of the work carried out and/or results. The relevance of the essentials driven on the basis of discussion(s) will be emphasized!

According to your advice, the conclusion was modified in the revised manuscript. (p.9L20-L27)

The other revised sentences were marked with red letter in the revised manuscript.

We hope that the revised manuscript will be suitable for the publication.

Dr. Masahiko Matsumiya,

Graduate School of Environment and Information Sciences,

Yokohama National University

E-mail/matsumiya-masahiko-dh@ynu.ac.jp

Thank you for sending many useful comments.

According to your comments, the revised manuscript was corrected as follows.

P3, L12 and L18: It's not clear what the authors mean with negative pressure on both these lines. Especially as the 0.1 MPa is 1 bar pressure.

According to your comments, the expression of the pressure was modified in the revised manuscript. (p.3L18)

P4, L8: Considering that the authors are using ADF, a STO basis set code, it's really surprising that they chose such small basis sets for their Gaussian09 calculations. Is there a reason for choosing only a DZ basis set? Especially as they use a TZ basis set for the latter ADF calculations.

As you pointed out, it would be better to adopt the large basis sets. In ADF simulations, STO is more exactly than GTO and all-electron and frozen-core basis sets are available for all elements. From a standpoint of balance for the precision and the computational cost, the basis-set is selected in this study. Similar simulation analysis was previously adopted in *J. Mol. Liq.*, **215** (2016) 308-315.

P4, L13: Only the cis-version of the NTf_2 molecule was used for the cluster calculations. Was there no exploration of the conformational equilibrium in for these complexes? If not, could the authors provide their reasoning?

According to your advice, the comment of the conformational equilibrium was added in the revised manuscript. (p.6L15-L20) Moreover, the conformational equilibrium in complexes is explained as follows. The equilibrium constant (K_{iso}) for the $[NTf_2]^-$ conformational isomerism from *trans*-$[NTf_2]$ and *cis*-$[NTf_2]$ is generally defined as $K_{iso}=c_{cis}/c_{trans}$.

$$K_{iso}$$

$$trans\text{-}[NTf_2] \Leftrightarrow cis\text{-}[NTf_2]$$
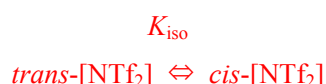
From the relation of $I=Jc$ (I is Raman intensity and J is Raman scattering coefficient), $K_{iso}=c_{cis}/c_{trans}=I_{cis}/I_{trans}\cdot J_{trans}/J_{cis}$. As shown in Fig.3, I_{cis} is always larger than I_{trans} at 298-398K and that means $I_{cis}>I_{trans}$. Then, from a standpoint of the thermodynamics, $\Delta_{iso}G=-RT\ln K_{iso}=-RT\ln c_{cis}/c_{trans}$, the term of $-RT\ln c_{cis}/c_{trans}$ is expressed as follows.

$-RT\ln c_{cis}/c_{trans}=-RT(\ln I_{cis}/J_{cis}-\ln I_{trans}/J_{trans})=-RT(\ln I_{cis}-\ln J_{cis}-\ln I_{trans}+\ln J_{trans})$

$=-RT(\ln I_{cis}-\ln I_{trans}+\ln J_{trans}-\ln J_{cis})=-RT(\ln I_{cis}/I_{trans}+\ln J_{trans}/J_{cis})$

From the thermodynamics relation, $\Delta_{iso}G=\Delta_{iso}H-T\Delta_{iso}S=-RT(\ln I_{cis}/I_{trans}+\ln J_{trans}/J_{cis})$

$\rightarrow-RT\ln(I_{cis}/I_{trans})=\Delta_{iso}H-T\Delta_{iso}S+RT\ln(J_{trans}/J_{cis})\rightarrow-RT\ln(I_{cis}/I_{trans})=\Delta_{iso}H-T\Delta_{iso}S-RT\ln(J_{cis}/J_{trans})$

$\rightarrow-R\ln(I_{cis}/I_{trans})=\Delta_{iso}H/T-\Delta_{iso}S-R\ln(J_{cis}/J_{trans})$

As a result, the J_{cis}/J_{trans} ratio is determined to be 0.68 experimentally and J_{trans}/J_{cis} is 1/0.68=1.47 ($J_{trans}/J_{cis}>1$). From the above relation ($I_{cis}>I_{tans}$ and $J_{trans}/J_{cis}>1$), the equilibrium constant is derived to be $K_{iso}=c_{cis}/c_{trans}>1$ and this result means $c_{cis}>c_{trans}$. Therefore, the cluster calculation of *cis*-$[NTf_2]$

is applied in this study, because the *cis*-[NTf$_2$] conformer is predominant and thermodynamically more stable.

On P5, the authors claim that the frequency mode of the NTf$_2$ that interacts with the metal ion is always at the same value, i.e. 751 cm^{-1}. Is that a reasonable approximation? Shouldn't the differing metal ions have a slightly different wavenumber value? (Especially as the authors mention later on that the calculated structures all have the same structures, yet should not have the same weighted mass of the frequency mode) or are they too close to tell apart with experimental setup?

As you pointed out, the metal ions would have a slightly different wavenumber value. In the case of similar iron group metals in this study, the similar results for Co(II) and Ni(II) in [EMI][TFSA] system were reported in *Anal. Sci.*, **24** (2008) 1377-1380. Then, the overlapping Raman bands were deconvoluted into individual components using a pseudo-Voigt function by nonlinear least-square analysis. The used pseudo-Voigt function was also adopted by *J. Phys. Chem. B*, **114** (2010) 6513-6521. Therefore, it is a reasonable approximation in this study.

Fig. 1

b) There is a noticeable frequency shift in the purple trace of this graph (a shift of maybe 1-2 cm^{-1}). Thus, there is the question if something else has started to happen inside this system.

As you pointed out, the deconvoluted data with a deviation of 1-2 cm^{-1} would be obtained. However, there is no something else to happen inside this Raman system. If a something else happens inside Raman system, the Raman spectrum definitely becomes strange.

c)The blue peak at 750 cm^{-1} seems to be far broader than the other peak. Is there a reason for that? Especially as the purple peak is sharper and in-line with the other peaks.

As you pointed out, the deconvoluted data with a broader peak would be obtained. Although we do not know a clear reason, it would depend on the original data before deconvolution. However, the Raman spectroscopy is normal state and the adopted pseudo-Voigt function is appropriate in this study.

The other revised sentences were marked with red letter in the revised manuscript.

We hope that the revised manuscript will be suitable for the publication.

Dr. Masahiko Matsumiya,

Graduate School of Environment and Information Sciences,

Yokohama National University

E-mail/matsumiya-masahiko-dh@ynu.ac.jp

Highlights

・The solvation structures of Fe(II), Co(II) and Ni(II) in ILs were investigated by Raman spectroscopy.

・The thermodynamic properties for the isomerism of $[NTf_2]^-$ from *trans*- to *cis*-isomer were evaluated.

・The bonding energies of $[M^{(II)}(cis\text{-}NTf_2)_3]^-$, (M=Fe, Co, Ni) were estimated from DFT calculations.

1

2

3

4

5

6

7 Solvation structure for Fe(II), Co(II) and Ni(II) complexes in $[P_{2225}][NTf_2]$ ionic liquids

8 investigated by Raman spectroscopy and DFT calculation

9

10 Yusuke TSUCHIDA[1], Masahiko MATSUMIYA[1*] and Katsuhiko TSUNASHIMA[2]

11

12

13 [1]Graduate School of Environment and Information Sciences, Yokohama National University,

14 79-2 Tokiwadai, Hodogaya-ku, Yokohama, 240-8501, JAPAN

15 [2]Department of Applied Chemistry and Biochemistry, National Institute of Technology, Wakayama College,

16 77 Noshima, Nada-cho, Gobo, Wakayama, 644-0023, JAPAN

17

18

19

20

21

22

23

24

* Corresponding author, Tel & Fax: +81-45-339-3464
 E-mail: matsumiya-masahiko-dh@ynu.ac.jp

1 **ABSTRACT**

2   The solvation structures of divalent iron, cobalt and nickel complexes in the ionic liquid, triethyl-*n*-

3 pentylphosphonium bis(trifluoromethyl sulfonyl) amide ($[P_{2225}][NTf_2]$) were investigated by Raman spectroscopy.

4 Based on a conventional analysis, the solvation numbers of Fe(II), Co(II), and Ni(II) in $[P_{2225}][NTf_2]$ were

5 determined to be 3.18, 3.21, and 3.14 at 298 K and 3.24, 3.32, and 3.37 at 373 K, respectively.

6   From the temperature dependence of the Raman bands the isomerism of $[NTf_2]^-$ from *trans*- to *cis*-

7 coordinated isomer in the bulk and the first solvation sphere of the central M^{2+} (M=Fe, Co, and Ni) cation in

8 $[P_{2225}][NTf_2]$, thermodynamic properties such as $\Delta_{iso}G$, $\Delta_{iso}H$, and $\Delta_{iso}S$ for the isomerism were evaluated. It was

9 revealed that *cis*-$[NTf_2]^-$ isomers were stabilized by enthalpic contribution, because $\Delta_{iso}H(M)$ became remarkably

10 negative in the first solvation sphere of the M^{2+} cation. Moreover, $\Delta_{iso}H(M)$ contributed to the remarkable decrease

11 in $\Delta_{iso}G(M)$, and this result clearly indicates that *cis*-$[NTf_2]^-$ conformers bound to M^{2+} cations are the preferred

12 coordination state of $[M^{(II)}(cis\text{-}NTf_2)_3]^-$ in $[P_{2225}][NTf_2]$.

13   The optimized geometries and the binding energies of $[Fe^{(II)}(cis\text{-}NTf_2)_3]^-$, $[Co^{(II)}(cis\text{-}NTf_2)_3]^-$, and $[Ni^{(II)}(cis\text{-}$

14 $NTf_2)_3]^-$ clusters were calculated by ADF simulations. The bonding energy, ΔE_b, was calculated as $\Delta E_b =$

15 $E_{tot}(cluster) - E_{tot}(M^{2+}) - nE_{tot}([NTf_2]^-)$, and ΔE_b ($[Fe^{(II)}(cis\text{-}NTf_2)_3]^-$), $\Delta E_b([Co^{(II)}(cis\text{-}NTf_2)_3]^-)$, and $\Delta E_b([Ni^{(II)}(cis\text{-}$

16 $NTf_2)_3]^-$) were calculated to be -2132.1 ± 6.4, -2254.6 ± 6.1, and -2283.4 ± 7.2 kJ mol^{-1}, respectively.

17 Furthermore, the bond distances of these clusters were consistent with the thermodynamic properties.

18

19 **Keywords:** Coordination state, DFT calculation, Iron group metal, Raman spectroscopy, Thermodynamic property

20

21

22

23

24

25

26

27

28

1. Introduction

Iron group elements are indispensable in high-tech industries due to their metallic properties [1,2]. In particular, Nd-Fe-B permanent magnets are finding increasing applications in a broad range of fields and are used for a variety of industrial products, such as voice coil motors, magnetic resonance imaging, and hybrid-type electric vehicles [3–5]. For the development of recycling process of Nd-Fe-B components, it is very important to establish a novel recovery process with energy-saving. For this purpose, we have previously demonstrated an electrodeposition method for Fe[6,7], Nd [7–12] and Dy [13,14] metals using room-temperature ionic liquids (RTILs) with the bis(trifluoromethyl sulfonyl)amide, $[NTf_2]^-$, anion. RTILs have several distinctive properties such as low vapor pressures, incombustibility, high ionic conductivity, and a wide electrochemical window [15,16]. In particular, phosphonium ILs containing the $[NTf_2]^-$ anion are appropriate for the electrodeposition of metals because of their low viscosities, high thermal stabilities, and wide electrochemical windows in comparison with imidazolium-based ILs [17].

In general, in ILs, metal ions are solvated by several molecular dipoles to form metal ion solvated clusters [18]. The electrodeposition process is affected significantly by the solvation structure of the metal ions in the ILs. There have been some reports concerning the solvation structures of various metal ions, Li [19–23], Mn [24,25], Fe [26], Co [24,26], Ni [24,26], Zn [24], Pr[27], Nd [10,27,28], Eu [29], and Dy [27,30], in NTf_2-based ILs as determined by Raman spectroscopy. However, there have been few reports concerning the analysis of the solvation structures at elevated temperatures or thermodynamic analyses concerning the isomerism of the $[NTf_2]^-$ anion, which can isomerize between *trans* and *cis* isomers in the bulk and in the first solvation sphere of the iron group metal ions dissolved in ILs. Therefore, we investigated the solvation number at elevated temperature and the isomerization characteristics of the $[NTf_2]^-$ ligands of Fe(II), Co(II), and Ni(II) complexes by investigating the temperature dependence of the Raman bands. In addition, DFT calculations were carried out using the Amsterdam Density Functional (ADF) program (version 2014.01) [31–35], and we have used these results to discuss the optimum geometries of these complexes in depth. The ADF package enables us to perform full-electron calculations for all elements including the heavy metal elements.

Therefore, by combining an experimental approach and computational analysis, we have gained a thorough understanding of the coordination states of iron group metal complexes in ILs. In this work, the solvation number and the $[NTf_2]^-$ isomer analysis of Fe(II), Ni(II), and Co(II) complexes in NTf_2-based ILs were investigated by

1   band intensity analysis and thermodynamic analysis using Raman spectroscopy. Moreover, the optimum geometries

2   and the bonding energies of these complexes were also examined using the ADF package to understand the stability

3   of their coordination states.

4

5   2. Experimental

6   2.1. Preparation

7   The phosphonium IL, triethyl-*n*-pentyl phosphonium bis(trifluoromethyl sulfonyl)amide, $[P_{2225}][NTf_2]$ was

8   prepared according to a well-documented procedure [36]. The $[P_{2225}][NTf_2]$ was synthesized by the ion exchange

9   between $[P_{2225}]Br$ (Nippon Chemical Industrial Co., Ltd., > 99.5 %) and $Li[NTf_2]$ (Kanto Chemical Co., Inc.,

10   99.7 %). Then, the generated $[P_{2225}][NTf_2]$ was purified by removing residual bromide ion with distilled water until

11   no AgBr precipitate was detected in the organic phase by titration with $AgNO_3$. The organic phase was dried under

12   vacuum < -0.1 MPa at 393 K for 48 h.

13       $Fe(NTf_2)_2$, $Ni(NTf_2)_2$, and $Co(NTf_2)_2$ salts were synthesized by a neutralization reaction between iron powder

14   (Wako Chemical Industries Ltd, 99.9%), $CoCO_3$ (Wako Pure Chemical Industries Ltd), $NiCO_3 \cdot 4H_2O$ (Wako Pure

15   Chemical Industries Ltd), and 1,1,1-trifluoro-*N*-[(trifluoromethyl)sulfonyl] methanesulfonamide ($H[NTf_2]$, Kanto

16   Chemical Co., Inc., > 99.8 %) in aqueous solution at 423 K for 20 min under stirring. The insoluble substance in

17   the reaction mixture was removed by filtration and the filtrate was evaporated at 393 K. The obtained $Fe(NTf_2)_2$,

18     $Co(NTf_2)_2$, and $Ni(NTf_2)_2$ salts were dried in vacuo (< 1.0×10^{-6} atm) at 393 K for 24 h.

19

20   2.2. Raman spectroscopy

21   The six solutions containing Fe(II), Co(II), and Ni(II) were prepared for the analysis of solvation number.

22   Appropriate amounts of $Fe(NTf_2)_2$, $Co(NTf_2)_2$, and $Ni(NTf_2)_2$ salts were dissolved in $[P_{2225}][NTf_2]$ at

23   concentrations of 0.23, 0.30, 0.38, 0.45, 0.53 and 0.59 mol kg^{-1}, respectively. Raman spectra (NRS-4100, JUSCO

24   Corp.) were measured at 298 and 373 K using a 532-nm laser. The appropriate gratings for the collection of the

25   Raman spectra were 1800 mm^{-1} and the selection of the gratings is based on the results of our recent investigations

26   [26,27].

27   Regarding the analysis of isomerism thermodynamics, the molar fractions of M(II) in the sample solutions,

28     $x_{M(II)}$, were 0.000, 0.033, 0.055, and 0.075. Raman spectra were measured at various temperatures, i.e., 298, 323,

1 348, 373, and 398 K. All Raman spectra were measured by accumulating 512 individual measurements to improve

2 the signal-to-noise ratio. The overlapping Raman bands were deconvoluted into individual components using a

3 pseudo-Voigt function.

4

5 **2.3. Calculation methods**

6   DFT calculations of the cation and anion components of the $[P_{2225}][NTf_2]$ ILs were carried out using the

7 Gaussian09 program [37]. The DFT calculations on models of the $[P_{2225}]^+$ and $[NTf_2]^-$ ions were performed at the

8 B3LYP/6-31G(d,p) [38-42] and B3LYP/6-31+G(d) level, respectively. Subsequently, frequency analysis was

9 carried out on the optimized geometries. The hybrid functional B3LYP, which includes a mixture of Hartree-Fock

10 exchange and DFT exchange-correlation, is Becke's three-parameter hybrid method (B3) [43] with non-local

11 correlation provided by the Lee, Yang, and Parr (LYP) functional [44]. The 6-31G basis set with diffuse and

12 polarization functions was used for all atoms.

13   The geometry optimizations of $[Fe^{(II)}(cis\text{-}NTf_2)_3]^-$, $[Co^{(II)}(cis\text{-}NTf_2)_3]^-$, and $[Ni^{(II)}(cis\text{-}NTf_2)_3]^-$ were performed

14 using the Amsterdam Density Functional (ADF) program [37]. The BP (Becke88-Perdew86 functional [45–48])

15 and TZP basis sets were applied for divalent iron group metals. The BP/DZP basis sets were used for light elements.

16 In ADF simulations, Slater-type orbitals (STO), which describe atomic orbitals more exactly than the Gaussian

17 orbitals (GTO) were used in Gaussian09. Moreover, all-electron and frozen-core basis sets are available for all

18 elements including iron group metals on the basis of the Zeroth-Order Regular Approximation (ZORA) method

19 [49–51]. The frozen-core approximation is effective to reduce the calculation time for systems with heavy nuclei.

20

21 **3 Results and discussion**

22 **3.1. Analysis of the solvation number**

23   The concentration dependences of the deconvoluted Raman spectra in the frequency range 720–780 cm^{-1} for

24 Fe(II), Co(II), and Ni(II) samples in $[P_{2225}][NTf_2]$ are shown in **Figs. 1(a)**, **1(b)**, and **1(c)**, respectively. Raman

25 spectra in this range were separated into two components, one at approximately 740 cm^{-1} and the other at 751 cm^{-1}.

26 The Raman bands can be attributed to the combination of stretching, ν_s(SNS), and bending vibrations, δ_s(CF$_3$), of

27 the $[NTf_2]^-$ anion [52,53]. These two bands at 740 and 751 cm^{-1} arise from the free $[NTf_2]^-$ anion and the $[NTf_2]^-$

28 anion bound to the metal ion, respectively. As can be seen from **Fig. 1**, a new band at 751 cm^{-1} is present as a

4

1   shoulder of the band at 740 cm^{-1}. This new band intensified with increasing concentration of M(II) in the IL. The

2   solvation number of M(II) in [P$_{2225}$][NTf$_2$] was evaluated using an analysis method similar to that suggested by

3   Umebayashi et al. [20,21]. The intensity of the deconvoluted Raman band of free [NTf$_2$]$^-$ anions in the bulk IL is

4   represented as $I_f = J_f c_f$, where J_f and c_f are the molar Raman scattering coefficient and the concentration of free

5   [NTf$_2$]$^-$ anions in the bulk, respectively. The c_f value is calculated as $c_f = c_T - c_b = c_T - nc_M$, where c_T, c_b, c_M, and n

6   express the concentration of total [NTf$_2$]$^-$ anions, that of bound [NTf$_2$]$^-$ anions (solvated to the metal ion), that of

7   metal ion, and the solvation number of the metal ion, respectively. By inserting $c_f = c_T - c_b = c_T - nc_M$ into $I_f = J_f c_f$,

8   the following equation is obtained:

9

10 $$I_f/c_M = J_f \times (c_T/c_M - n). \tag{1}$$

11

12   The plot of I_f/c_M against c_T/c_M yields a straight line if the solvation number of M(II) cation in [P$_{2225}$][NTf$_2$] is

13   constant. Thus, n is obtained using $n = -\beta/\alpha$ from the slope of $\alpha = J_f$ and the intercept of $\beta = -J_f n$. The plots of I_f/c_M

14   against c_T/c_M for [P$_{2225}$][NTf$_2$] ILs containing 0.23–0.59 mol kg^{-1} of Fe(II), Co(II), and Ni(II) are shown in **Figs.**

15   **2(a)**, **2(b)** and **2(c)**, respectively. As shown in these plots at 373 K, the strong linear relationship indicates that the

16   number of [NTf$_2$]$^-$ anion solvated to M(II) remained unchanged under the examined experimental conditions.

17   Hence, the values of n of Fe(II), Co(II), and Ni(II) in ILs were evaluated as $n_{Fe(II)} = 3.18$, $n_{Co(II)} = 3.21$, and

18     $n_{Ni(II)} = 3.14$ at 298 K, and $n_{Fe(II)} = 3.24$, $n_{Co(II)} = 3.32$, and $n_{Ni(II)} = 3.37$ at 373 K, respectively. This result indicates

19   that the M^{2+} cations in [P$_{2225}$][NTf$_2$] were solvated by five [NTf$_2$]$^-$ anions; therefore, [M$^{(II)}$(NTf$_2$)$_3$]$^-$ clusters were

20   present in this system.

21

22   **3.2. Thermodynamic stability for [NTf$_2$]$^-$ isomerism**

23   The effect of temperature on the Raman spectra of the M(II) ions in [P$_{2225}$][NTf$_2$] ($x_{M(II)}$ = 0.000, 0.033, 0.055,

24   and 0.075) was investigated to evaluate the thermodynamic stability of the [NTf$_2$]$^-$ complex isomers. The

25   temperature dependence of the deconvoluted Raman spectrum for (a) Fe(II), (b) Co(II), and (c) Ni(II) in

26   [P$_{2225}$][NTf$_2$] ($x_{M(II)}$ = 0.033) in the frequency range of 370–440 cm^{-1} is shown in **Fig. 3**. Two peaks are visible in

27   Fig. 3, and these are suitable for the thermodynamic analysis of the [NTf$_2$]$^-$ isomer because no Raman bands arising

28   from [P$_{2225}$]$^+$ are predicted to overlap [NTf$_2$]$^-$ bands in the range of 370–440 cm^{-1} [30]. The wagging ω-SO$_2$

1   vibration at 396 and 403 cm^{-1} shown in Fig. 3 correspond to *trans*-[NTf$_2$]$^-$ and *cis*-[NTf$_2$]$^-$ isomers, respectively

2   [21]. Regarding the temperature dependence of the Raman spectra for neat [P$_{2225}$][NTf$_2$], the Raman intensity of the

3   *trans*-[NTf$_2$]$^-$ Raman band was larger than that of *cis*-[NTf$_2$]$^-$. This result indicates that *trans*-[NTf$_2$]$^-$ isomers are

4   enthalpically stable compared to *cis*-[NTf$_2$]$^-$ isomers. Regarding the Raman band of M(II) in [P$_{2225}$][NTf$_2$] at $x_{M(II)}$ =

5   0.033 shown in Fig. 3, the peak area of the band arising from *cis*-isomers increased in comparison with the that

6   arising from neat [P$_{2225}$][NTf$_2$]. This result indicates that the [NTf$_2$]$^-$ anions solvating in M(II) are predominantly

7   coordinated as *cis*-isomers. That is to say, when [NTf$_2$]$^-$ is bound to M(II) in [P$_{2225}$][NTf$_2$], *cis*-[NTf$_2$]$^-$ isomers are

8   more energetically stable than the *trans*-[NTf$_2$]$^-$ isomers.

9   To perform a quantitative evaluation based on the thermodynamics of the [NTf$_2$]$^-$ isomers, the apparent

10   thermodynamic quantities; $\Delta_{iso}G$, $\Delta_{iso}H$, and $T\Delta_{iso}S$ were determined from analysis of Van't Hoff plots [20]. The

11   parameters $\Delta_{iso}G$, $\Delta_{iso}H$, and $T\Delta_{iso}S$ derived for *trans*-[NTf$_2$]$^-$ to *cis*-[NTf$_2$]$^-$ as a function $x_{M(II)}$ can be defined by

12   Eq. (2). As the first step, the apparent equilibrium constant, K_{iso} for the [NTf$_2$]$^-$ conformational isomerism from the

13   *trans*-[NTf$_2$]$^-$ to *cis*-[NTf$_2$]$^-$ as a function $x_{M(II)}$ was defined as $K_{iso} = c_{cis}/c_{trans}$.

14

15 K_{iso}

16   *trans*-[NTf$_2$] $\Leftrightarrow$ *cis*-[NTf$_2$]   (2)

17

18   From the relation of $I=Jc$ (*I* is Raman intensity and *J* is Raman scattering coefficient), $K_{iso}=I_{cis}/I_{trans}\cdot J_{trans}/J_{cis}$. As

19   shown in Fig.3, this result implies $I_{cis}>I_{trans}$ and the *cis*-[NTf$_2$] conformer would be predominant in [P$_{2225}$][NTf$_2$]

20   system. Therefore, from a stand point of thermodynamics, the conformational isomerism was discussed as follows.

21   Using this equilibrium constant, $\Delta_{iso}G$ was calculated as follows:

22

23                  $\Delta_{iso}G = -RT \ln K_{iso} = -RT \ln (c_{cis}/c_{trans})$,   (3)

24

25   where *R* and *T* are the gas constant and the absolute temperature, respectively. In addition, $\Delta_{iso}G$ can be expressed

26   as $\Delta_{iso}G = \Delta_{iso}H - T\Delta_{iso}S$, and the Raman intensity, *I*, is $I = Jc$. When these two equations are substituted for

27     $\Delta_{iso}G = -RT \ln (c_{cis}/c_{trans})$, the following Van't Hoff equation [20] is obtained:

28

1 $$-R\ln(I_{cis}/I_{trans}) = \Delta_{iso}H/T - \Delta_{iso}S - R\ln(J_{cis}/J_{trans}) \tag{4}$$

2

3 where I_{cis} and I_{trans} are the Raman intensities of cis-$[NTf_2]^-$ and trans-$[NTf_2]^-$ isomers, respectively. J_{cis} and J_{trans} are

4 the Raman scattering coefficients for the cis-$[NTf_2]^-$ and trans-$[NTf_2]^-$ isomers. The corresponding Van't Hoff plots

5 are shown in **Fig. 4**, and these are derived from the ratio of Raman band intensities for cis-$[NTf_2]^-$ and trans-

6 $[NTf_2]^-$ isomers at 396 and 403 cm^{-1}, based on Eq. (4). Similar measurements were performed for samples with

7 different values of $x_{M(II)}$ (e.g., $x_{M(II)}$= 0.000, 0.033, 0.055, and 0.075) and the corresponding plots are also shown in

8 Fig. 4. The Van't Hoff plots show good linear relationships at all $x_{M(II)}$ concentrations, and the concentration

9 dependence is clearly demonstrated by the slopes of the plots. This indicates that the slopes of the plots, which

10 represent $\Delta_{iso}H$, can be evaluated as a function of $x_{M(II)}$ with high accuracy. In addition, we found that the slope of

11 the plots (= $\Delta_{iso}H$) decreased with increasing M(II) concentration. This result indicates that cis-$[NTf_2]^-$ was

12 thermodynamically more stable than trans-$[NTf_2]^-$ in the system with a high concentration of M(II), and cis-$[NTf_2]^-$

13 anions are the major isomers coordinated to the M^{2+} cations.

14 In addition, the value of $\Delta_{iso}S$ was evaluated from the intercept of the Van't Hoff plot based on Eq. (4). For

15 this, the J_{cis}/J_{trans} ratio must be considered, and this value was estimated using the relationship $I_{cis} = -$

16 $(J_{cis}/J_{trans}) I_{trans} + J_{cis}c_T$ [20]. From the slope of the plots of I_{trans} against I_{cis}, we experimentally determined that the

17 value of J_{cis}/J_{trans} ratio was 0.68. To confirm the accuracy of this value (0.68), we estimated the value of the

18 J_{cis}/J_{trans} ratio using DFT calculations. The theoretical value of the J_{cis}/J_{trans} ratio calculated at the B3LYP/6-

19 31+G(d) level of theory was 0.69. Thus, the experimental value agrees well with that predicted by theory; therefore,

20 we used the J_{cis}/J_{trans} ratio to evaluate the entropy term, $\Delta_{iso}S$. Then, from the obtained values of $\Delta_{iso}H$ and $\Delta_{iso}S$,

21 $\Delta_{iso}G$ (= $\Delta_{iso}H - T\Delta_{iso}S$) at 298 K was estimated, as described above. All thermodynamic quantities (i.e., $\Delta_{iso}G$,

22 $\Delta_{iso}H$, and $T\Delta_{iso}S$) at each value of $x_{M(II)}$ are tabulated in **Table 1**, and these values are also plotted against $x_{M(II)}$, as

23 shown in **Fig. 5**. It can be inferred from the linearity of these plots that the thermodynamic quantities; $\Delta_{iso}X$ ($X = G$,

24 H, and S) are a function of $x_{M(II)}$. It appears that the apparent thermodynamic quantities are the sum of those of the

25 free $[NTf_2]^-$ anions in the bulk, $[\Delta_{iso}X(bulk)]$, and those which derived from the ligated $[NTf_2]^-$ anions in the first

26 solvation sphere of the central $[M^{2+}]$ cation, $[\Delta_{iso}X(M^{2+})]$. That is to say, the apparent thermodynamic quantities,

27 $\Delta_{iso}X$ ($X=G$, H, and S), can be expressed by the following equation [20]:

28

$$\Delta_{\text{iso}}X = nx_{\text{M(II)}} \, \Delta_{\text{iso}}X(M^{2+}) + (1 - nx_{\text{M(II)}}) \, \Delta_{\text{iso}}X(\text{bulk}), \tag{5}$$

where n stands for the solvation number of M(II), $n = 3.0$. Therefore, based on Eq. (5), the values of $\Delta_{\text{iso}}X$ at $x_{\text{M(II)}} = 0$ and 0.50 are $\Delta_{\text{iso}}X(\text{bulk})$ and $\Delta_{\text{iso}}X(M^{2+})$, respectively, as shown with the broken and chain lines in **Fig. 5**. Thermodynamic quantities for $[NTf_2]^-$ of the bulk and the first solvation sphere of the M^{2+} cation are listed in **Table 1**. Regarding the bulk condition, the obtained values of $\Delta_{\text{iso}}G(\text{bulk})$, $\Delta_{\text{iso}}H(\text{bulk})$, and $T\Delta_{\text{iso}}S(\text{bulk})$ at 298 K were -1.06, 6.86, and 7.92 kJ mol^{-1}, respectively. In this case, *trans*-$[NTf_2]^-$ makes a significant contribution to the total enthalpy as indicated by the positive value of $\Delta_{\text{iso}}H(\text{bulk})$ (6.86 kJ mol^{-1}). $T\Delta_{\text{iso}}S(\text{bulk})$ (7.92 kJ mol^{-1}) was also positive and slightly larger than that of $\Delta_{\text{iso}}H(\text{bulk})$, indicating that *cis*-$[NTf_2]^-$ is entropy-controlled in $[P_{2225}][NTf_2]$. As a result, the value of $\Delta_{\text{iso}}G(\text{bulk})$ suggests that *trans*-$[NTf_2]^-$ and *cis*-$[NTf_2]^-$ are almost at equilibrium in neat $[P_{2225}][NTf_2]$ because there is virtually no difference in the Gibbs free energies (-1.06 kJ mol^{-1}) of the *trans*-isomers and *cis*-isomers. In contrast, in the first solvation sphere of M^{2+}, *e.g.*, the value of $\Delta_{\text{iso}}H(\text{Fe})$ (-29.54 kJ mol^{-1}) increased to a very negative value, implying that *cis*-$[NTf_2]^-$ isomers were stabilized by enthalpic contributions. This value of $\Delta_{\text{iso}}H(\text{Fe})$ contributed to the remarkable decrease in the value of $\Delta_{\text{iso}}G(\text{Fe})$, which became negative (-7.53 kJ mol^{-1}) compared to that of $\Delta_{\text{iso}}G(\text{Fe})$. This result clearly showed that *cis*-$[NTf_2]^-$ bound to M^{2+} cation is preferred and that coordination of $[M^{(II)}(\textit{cis}\text{-}NTf_2)_3]^-$ is stable in $[P_{2225}][NTf_2]$. The stabilization of *cis*-$[NTf_2]^-$ bound to the central M^{2+} cation results from charge-dipole interactions between M^{2+} cations and *cis*-$[NTf_2]^-$ anions. The dipole moments of *trans*-$[NTf_2]^-$ and *cis*-$[NTf_2]^-$, estimated from DFT calculations at the B3LYP/6-31+G(d) level of theory, are 0.29 and 4.07, respectively. We believe that the *cis*-$[NTf_2]^-$ isomer has a relatively large electric charge-dipole interaction with M^{2+} ions, forming a stable solvation structure with *cis*-$[NTf_2]^-$ anions because their dipole moments are greater than those of *trans*-$[NTf_2]^-$ anions.

3.3. Geometry analysis of $[M^{(II)}(\textit{cis}\text{-}NTf_2)_3]^-$ clusters

As discussed in previous sections, the solvation number of Fe(II), Co(II), and Ni(II) cations in $[P_{2225}][NTf_2]$ is 3.0, and *cis*-$[NTf_2]^-$ anions are the predominant isomer coordinating the M^{2+} cations in the first solvation sphere. After geometry optimization of iron group metal clusters using DFT calculations as shown in **Fig. 6**, suitable initial geometries of the *cis*-$[NTf_2]^-$ anions have been found [30]. The scalar relativistic zero order regular approximation (ZORA) method allows inclusion of relativistic effects in heavy atoms at reduced computational cost [49–51], and

1 this was used for calculations on two clusters. In addition, the frozen-core approximation was also introduced to

2 reduce computational costs. In all of clusters, the oxygen atoms (O') bound to the M^{2+} cations were found to be

3 evenly distributed around the cations. The results indicated that the ligands were positioned so that the repulsion

4 energy between each ligand was minimized because the d-orbital do not have a significant stereochemical influence

5 on ligand geometries. As for the $[M^{(II)}(cis\text{-}NTf_2)_3]^-$ complex, three $[NTf_2]^-$ anions were bidentate ligands. As a

6 result, the coordination number of $[M^{(II)}(cis\text{-}NTf_2)_3]^-$ was 6. The coordination numbers of $[NTf_2]^-$ for Co^{2+} and Ni^{2+}

7 cations in 1-ethyl-3-methylimidazolium bis(trifluoromethylsulfonyl) amide; $[EMI][NTf_2]$ were also 3 [24], as

8 determined by Raman spectroscopic analysis and our results were consistent with previous report.

9 The bonding energy between the central M^{2+} cation and $[NTf_2]^-$ ligands; ΔE_b, was calculated as

10 $\Delta E_b = E_{tot}(\text{cluster}) - E_{tot}(M^{2+}) - nE_{tot}([NTf_2]^-)$, where n is solvation number of M^{2+} cations. The values thus

11 calculated were -2131.1 ± 6.4, -2254.6 ± 6.1, and -2283.4 ± 7.2 kJ mol^{-1} for $[Fe^{(II)}(cis\text{-}NTf_2)_3]^-$, $[Co^{(II)}(cis\text{-}$

12 $NTf_2)_3]^-$, and $[Ni^{(II)}(cis\text{-}NTf_2)_3]^-$ clusters, respectively. The errors were estimated from the calculation results based

13 on different basis-sets. Furthermore, we found that there were almost no differences among these bonding energies.

14 The bond distance, the bond angle, the dihedral angle and the dipole moment for the optimized geometries of

15 $[M^{(II)}(cis\text{-}NTf_2)_3]^-$ (M=Fe, Co and Ni) clusters were tabulated in **Table 2**. Although there were almost no

16 differences among these optimized structures, the dipole moment of the $[Ni^{(II)}(cis\text{-}NTf_2)_3]^-$ cluster was found to be

17 larger than that of the other clusters.

18

19 **4. Conclusion**

20 From the analysis of 740–751 cm^{-1} for Fe(II), Co(II), and Ni(II) samples by Raman spectroscopy, the number

21 of $[NTf_2]^-$ anions solvated to M^{2+} was found to be about 3.0 ; therefore, M^{2+} cations are present as $[M^{(II)}(NTf_2)_3]^-$

22 clusters in $[P_{2225}][NTf_2]$. Moreover, the thermodynamic stability of $[NTf_2]^-$ isomers was evaluated from Van't Hoff

23 plots of the temperature dependence of the Raman bands at temperatures ranging from 298 to 398 K. As for the

24 bulk condition, $\Delta_{iso}G(\text{bulk})$, $\Delta_{iso}H(\text{bulk})$, and $T\Delta_{iso}S(\text{bulk})$ at 298 K were determined to be -1.06, 6.86, and 7.92 kJ

25 mol^{-1}, respectively. These results indicate that $trans\text{-}[NTf_2]^-$ made a significant contribution to the enthalpy.

26 Furthermore, $cis\text{-}[NTf_2]^-$ was determined to be entropy-controlled in $[P_{2225}][NTf_2]$, because $T\Delta_{iso}S(\text{bulk})$ was

27 slightly larger than $\Delta_{iso}H(\text{bulk})$. In contrast, in the first solvation sphere of the $[M^{2+}]$ cations, $\Delta_{iso}H(M)$ became

28 significantly negative, indicating that $cis\text{-}[NTf_2]^-$ isomers are stabilized by enthalpy. $\Delta_{iso}H(M)$ contributed to the

9

remarkable decrease in the $\mathit{\Delta}_{iso}G(M)$, and this result indicates that cis-$[NTf_2]^-$ bound to M^{2+} cations was preferentially stabilized; consequently, the coordination state of $[M^{(II)}(cis\text{-}NTf_2)_3]^-$ became steady in $[P_{2225}][NTf_2]$

Furthermore, the optimum geometries and the bonding energies of $[Fe^{(II)}(cis\text{-}NTf_2)_3]^-$, $[Co^{(II)}(cis\text{-}NTf_2)_3]^-$, and $[Ni^{(II)}(cis\text{-}NTf_2)_3]^-$ were also determined by DFT simulations using the ADF package. The bonding energy, ΔE_b, was estimated by $\Delta E_b = E_{tot}(\text{cluster}) - E_{tot}(M^{2+}) - nE_{tot}([NTf_2]^-)$. Thus, $\Delta E_b([Fe^{(II)}(cis\text{-}NTf_2)_3]^-)$, $\Delta E_b([Co^{(II)}(cis\text{-}NTf_2)_3]^-)$, and $\Delta E_b([Ni^{(II)}(cis\text{-}NTf_2)_3]^-)$ were calculated to be -2132.1 ± 6.4, -2254.6 ± 6.1, and -2283.4 ± 7.2 kJ mol^{-1}, respectively. Finally, the structural information of the optimized these clusters were consistent with the thermodynamic properties.

References

[1] J. Yang, X. Li, J. Lang, L. Yang, M. Wei, M. Gao, X. Liu, H. Zhai, R. Wang, Y. Liu, J. Cao, Mater. Sci. Semicond. Process. 14 (2011) 247-252.

[2] D. Yuan, Y. Liu, Mater. Chem. Phys. 96 (2006) 79-83.

[3] N. Ono, M. Sagawa, R. Kasada, H. Matsui, A. Kimura, J. Magn. Magn. Mater. 323 (2011) 297-300.

[4] K. Miura, M. Itoh, K. Machida, J. Alloys Compd. 466 (2008) 228-232.

[5] Y. Matsuura, J. Magn. Magn. Mater. 303 (2006) 344-347.

[6] M. Matsumiya, T. Yamada, S. Murakami, Y. Kohno, K. Tsunashima, Solvent Extr. Ion Exch., 34(5) (2016) 454-468.

[7] H. Ota, M. Matsumiya, T. Yamada, T. Fujita, S. Kawakami, Sep. Purif. Technol., 170 (2016) 417-426.

[8] H. Kondo, M. Matsumiya, K. Tsunashima, S. Kodama, Electrochim. Acta 66(1) (2012) 313-319.

[9] H. Kondo, M. Matsumiya, K. Tsunashima, S. Kodama, ECS Trans. 50 (11) (2012) 529-538.

[10] N. Tsuda, M. Matsumiya, K. Tsunashima, S. Kodama, ECS Trans. 50 (11) (2012) 539-548.

[11] M. Ishii, M. Matsumiya, S. Kawakami, ECS Trans. 50 (11) (2012) 549-560.

[12] M. Matsumiya, M. Ishii, R. Kazama, S. Kawakami, Electrochim. Acta 146 (2014) 371-377.

[13] A. Kurachi, M. Matsumiya, K. Tsunashima, S. Kodama, J. Appl. Electrochem. 42 (11) (2012) 961-968.

[14] R. Kazama, M. Matsumiya, N. Tsuda, K. Tsunashima, Electrochim. Acta 113 (2013) 269-279.

[15] D.R. MacFarlane, M. Forsyth, P.C. Howlett, J.M. Pringle, J. Sun, G. Annt, W. Neil,E.I. Izgorodina, Acc. Chem. Res. 40 (2007) 1165-1173.

[16] M. Shamsipur, A.A.M. Beigi, M. Teymouri, S.M. Pourmortazavi, M.Irandoust, J. Mol. Liq. 157(1) (2010) 43-50.

[17] K. Tsunashima, A. Kawabata, M. Matsumiya, S. Kodama, R. Enomoto, M. Sugiya, Y. Kunugi, Electrochem. Commun. 13 (2011) 178-181.

[18] H. Ohtaki, T. Radnai, Chem. Rev. 93(3) (1993) 1157-1204.

[19] M. Herstedt, M. Smirnov, P. Johansson, M. Chami, J. Grondin, L. Servant, J.-C. Lassegues, J. Raman Spectrosc. 36 (2005) 762-770.

[20] Y. Umebayashi, S. Mori, K. Fujii, S. Tsuzuki, S. Seki, K. Hayamizu, S. Ishiguro, J. Phys. Chem. B 114 (2010) 6513-6521.

[21] Y. Umebayashi, T. Mitsugi, S. Fukuda, T. Fujimori, K. Fujii, R. Kanzaki, M. Takeuchi, S. Ishiguro, J. Phys. Chem. B 111 (2007) 13028-13032.

[22] A. Shirai, K. Fujii, S. Seki, Y. Umebayashi, S. Ishiguro, Y. Ikeda, Anal. Sci. 24 (2008) 1291-1296.

[23] J.-C. Lassegues, J. Grondin, C. Aupetit, P. Johansson, J. Phys. Chem. A 113 (2009) 305-314.

[24] K. Fujii, T. Nonaka, Y. Akimoto, Y. Umebayashi, S. Ishiguro, Anal. Sci. 24 (2008) 1377-1384.

[25] Y. Umebayashi, K. Matsumoto, Y. Mune, Y. Zhang, S. Ishiguro, Phys. Chem. Chem. Phys. 5 (2003) 2552-2556.

[26] M. Matsumiya, Y. Kamo, K. Hata, K. Tsunashima, J. Mol. Struct., 1048 (2013) 59-63.

[27] K. Kuribara, M. Matsumiya, K. Tsunashima, J. Mol. Struct., 1125 (2016) 186-192.

[28] M. Matsumiya, Application of Ionic Liquids on Rare Earth Green Separation and Utilization (2016) 117-153.

[29] M. Furlani, A. Ferry, A. Franke, P. Jacobsson, B.-E. Mellander, Solid State Ionics 113–115 (1998) 129-138.

[30] M. Matsumiya, R. Kazama, K. Tsunashima, J. Mol. Liq., 215 (2016) 308-315.

[31] G. te Velde, F. M. Bickelhaupt, E. J. Baerends, C. Fonseca Guerra, S. J. A. van Gisbergen, J. G. Snijders, T. Ziegler, J. Comput. Chem. 22 (2001) 931-967.

[32] C. Fonseca Guerra, J. G. Snijders, G. te Velde, E. J. Baerends, Theor. Chem. Acc. 99 (1998) 391-403.

1   [33] E.J. Baerends and P. Roos, Int. J. Quantum Chem. Symp. 12 (1978) 169-190.

2   [34] E.J. Baerends, D.E. Ellis, P. Ros, Chem. Phys. 2 (1973) 41-44.

3   [35] ADF2014.01, SCM, Theoretical Chemistry, Vrije Universiteit, Amsterdam, The Netherlands.

4   [36] K. Tsunashima, M. Sugiya, Electrochem. Commun. 9 (2007) 2353-2358.

5   [37] M.J. Frisch, G.W. Trucks, H.B. Schlegel, G.E. Scuseria, M.A. Robb, J.R. Cheeseman, G. Scalmani, V. Barone,

6   B. Mennucci, G.A. Petersson, H. Nakatsuji, M. Caricato, X. Li, H.P. Hratchian, A.F. Izmaylov, J. Bloino, G.

7   Zheng, J.L. Sonnenberg, M. Hada, M. Ehara, K. Toyota, R. Fukuda, J. Hasegawa, M. Ishida, T. Nakajima, Y.

8   Honda, O. Kitao, H. Nakai, T. Vreven, J.A. Montgomery, Jr., J.E. Peralta, F. Ogliaro, M. Bearpark, J.J. Heyd,

9   E. Brothers, K.N. Kudin, V.N. Staroverov, T. Keith, R. Kobayashi, J. Normand, K. Raghavachari, A. Rendell,

10   J.C. Burant, S.S. Iyengar, J. Tomasi, M. Cossi, N. Rega, J.M. Millam, M. Klene, J.E. Knox, J.B. Cross, V.

11   Bakken, C. Adamo, J. Jaramillo, R. Gomperts, R.E. Stratmann, O. Yazyev, A.J. Austin, R. Cammi, C. Pomelli,

12   J.W. Ochterski, R.L. Martin, K.Morokuma, V.G. Zakrzewski, G.A. Voth, P. Salvador, J.J. Dannenberg, S.

13   Dapprich, A.D. Daniels, O. Farkas, J.B. Foresman, J.V. Ortiz, J. Cioslowski, D.J. Fox, Gaussian, Inc.,

14   Wallingford CT, 2010.

15 [38] Pc. Harihara, J.A. Pople, Mol. Phys. 27 (1974) 209-214.

16 [39] R. Ditchfie, W.J. Hehre, J.A. Pople, J. Chem. Phys. 54 (1971) 724-728.

17 [40] M.M. Francl, W.J. Pietro, W.J. Hehre, J.S. Binkley, M.S. Gordon, D.J. Defrees, J.A. Pople, J. Chem. Phys.

18   77(7) (1982) 3654-3665.

19 [41] Pc. Harihara, J.A. Pople, Theor. Chim. Acta 28(3) (1973) 213-222.

20 [42] W.J. Hehre, R. Ditchfie, J.A. Pople, J. Chem. Phys. 56 (1972) 2257-2261.

21 [43] A.D. Becke, J. Chem. Phys. 98(7) (1993) 5648-5652.

22 [44] C. Lee, W. Yang, R.G. Parr, Phys. Rev. B 37 (1988) 785-789.

23 [45] S.H. Vosko, L. Wilk, M.C. Nusair, J. Phys. 58 (1980) 1200–1211.

24 [46] J.P. Perdew, Phys. Rev. B. 33 (1986) 8822–8824.

25 [47] A.D. Becke, Phys. Rev. A. 38 (1988) 3098–3100.

26 [48] J.C. Slater, Johnson KH. Phys. Rev. B. 5 (1972) 844-853.

27 [49] E. van Lenthe, E. J. Baerends, J. G. Snijders, J. Chem. Phys. 99 (1993) 4597-4610.

28 [50] S.G. Wang, D.K. Pan, W.H.E. Schwarz, J. Chem. Phys. 102 (1995) 9296-9308.

1   [51] S.G. Wang, W.H.E. Schwarz, J. Phys. Chem. 99(30) (1995) 11687-11695.

2   [52] I. Rey, P. Johansson, J. Lindgren, J. C. Lassegues, J. Grondin, and L. Servant, J. Phys. Chem. A, 102(19)

3   (1998) 3249-3258.

4   [53] M. Castriota, T. Caruso, R. G. Agostino, E. Cazzanelli, W. A. Henderson, and S. Passerini, J. Phys. Chem. A,

5   109(1) (2005) 92-96.

6

Caption of Figures

Fig. 1 Raman spectra of $[P_{2225}][NTf_2]$ containing 0.23, 0.30, 0.38, 0.45, 0.53 and 0.59 mol kg^{-1} (a) Fe(II), (b) Co(II) and (c) Ni(II) at 373 K.
Red line: 0.23 mol kg^{-1}, orange line: 0.30 mol kg^{-1}, yellow green line: 0.38 mol kg^{-1},
green line: 0.45 mol kg^{-1}, blue line: 0.53 mol kg^{-1}, purple line: 0.59 mol kg^{-1}

Fig. 2 Plot of I_f/c_M against c_T/c_M for $[P_{2225}][NTf_2]$ containing 0.23–0.59 mol kg^{-1} (a) Fe(II), (b) Co(II) and (c) Ni(II) at 373 K.

Fig. 3 Temperature dependence of the deconvoluted Raman spectrum of (a) Fe(II), (b) Co(II) and (c) Ni(II) ($x_{M(II)}$=0.033, M=Fe, Co and Ni) in $[P_{2225}][NTf_2]$ in the frequency range of 370-440 cm^{-1}.
Red line: 298 K, orange line: 323 K, green line: 348 K, blue line: 373 K, purple line: 398 K.

Fig. 4 Van't Hoff plot for the $[NTf_2]^-$ isomerism in $[P_{2225}][NTf_2]$ containing (a) Fe(II), (b) Co(II) and (c) Ni(II), ○: $x_{M(II)}$=0.000, ●: $x_{M(II)}$= 0.033, ▲: $x_{M(II)}$= 0.055 and ■: $x_{M(II)}$=0.075, (M=Fe, Co and Ni).

Fig. 5 Apparent thermodynamic properties of (a) Fe(II), (b) Co(II) and (c) Ni(II) in $[P_{2225}][NTf_2]$ for the conformational isomerism of $[NTf_2]^-$ from the *trans*- to *cis*-isomer as a function of $x_{M(II)}$ (M=Fe, Co and Ni) at 298 K.

Fig. 6 The optimized geometry for $[M^{(II)}(cis\text{-}NTf_2)_3]^-$ clusters calculated at the BD/DZP level using the TZP basis set for M^{2+}, (M=Fe, Co, Ni).
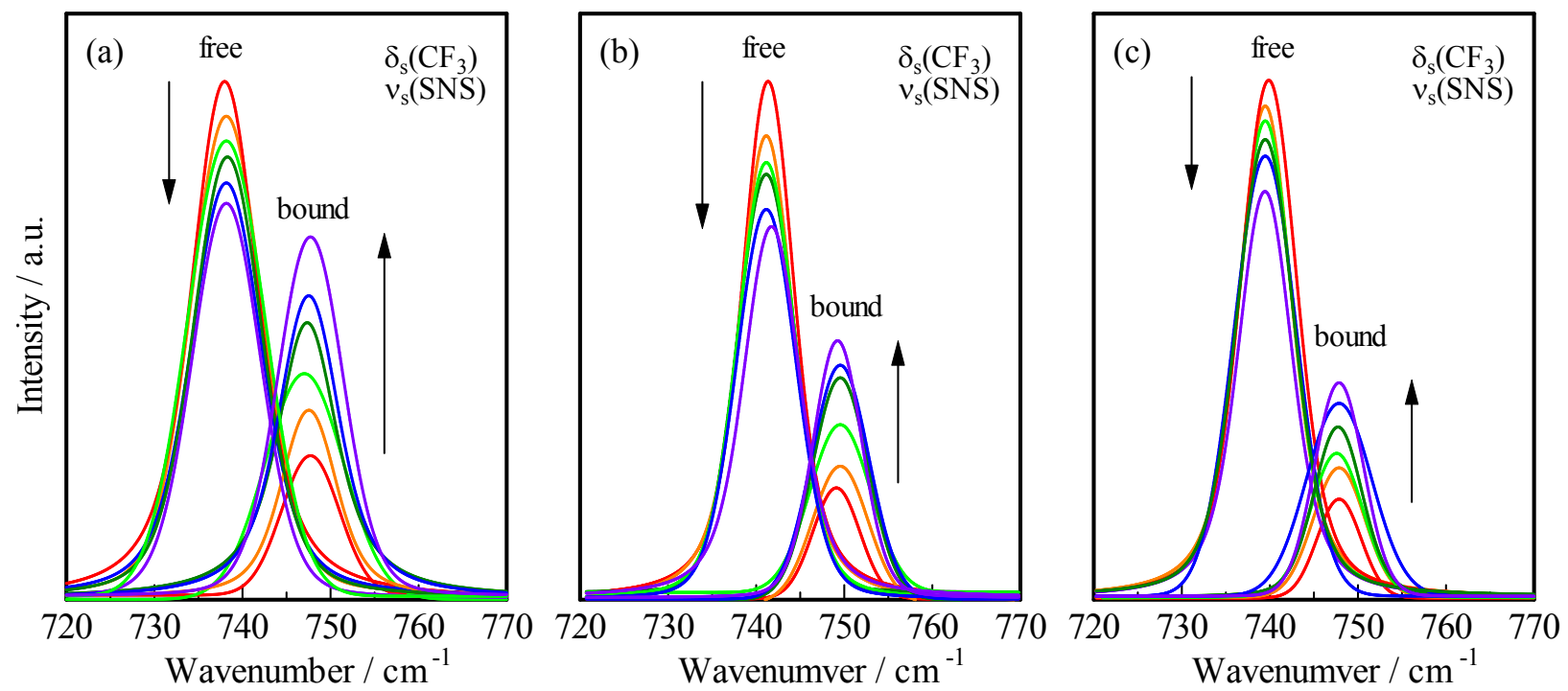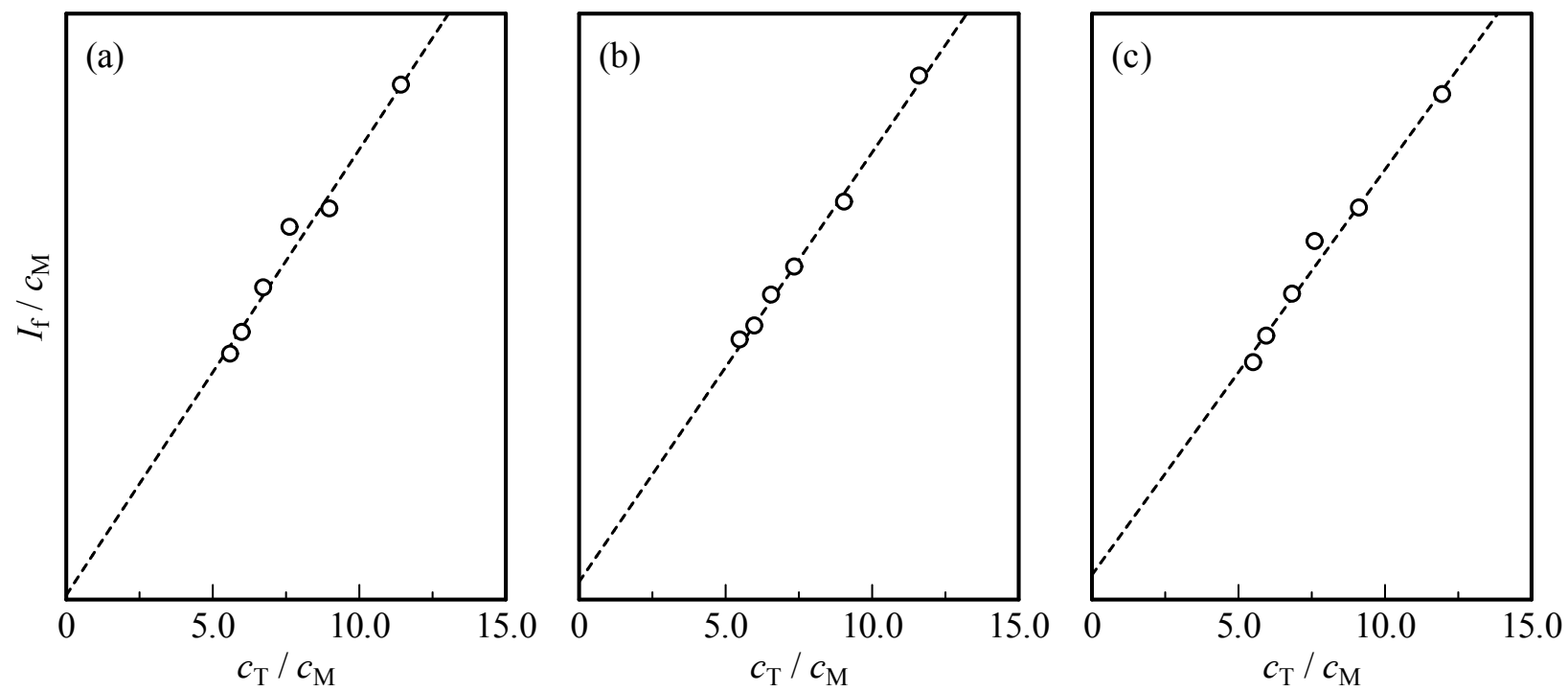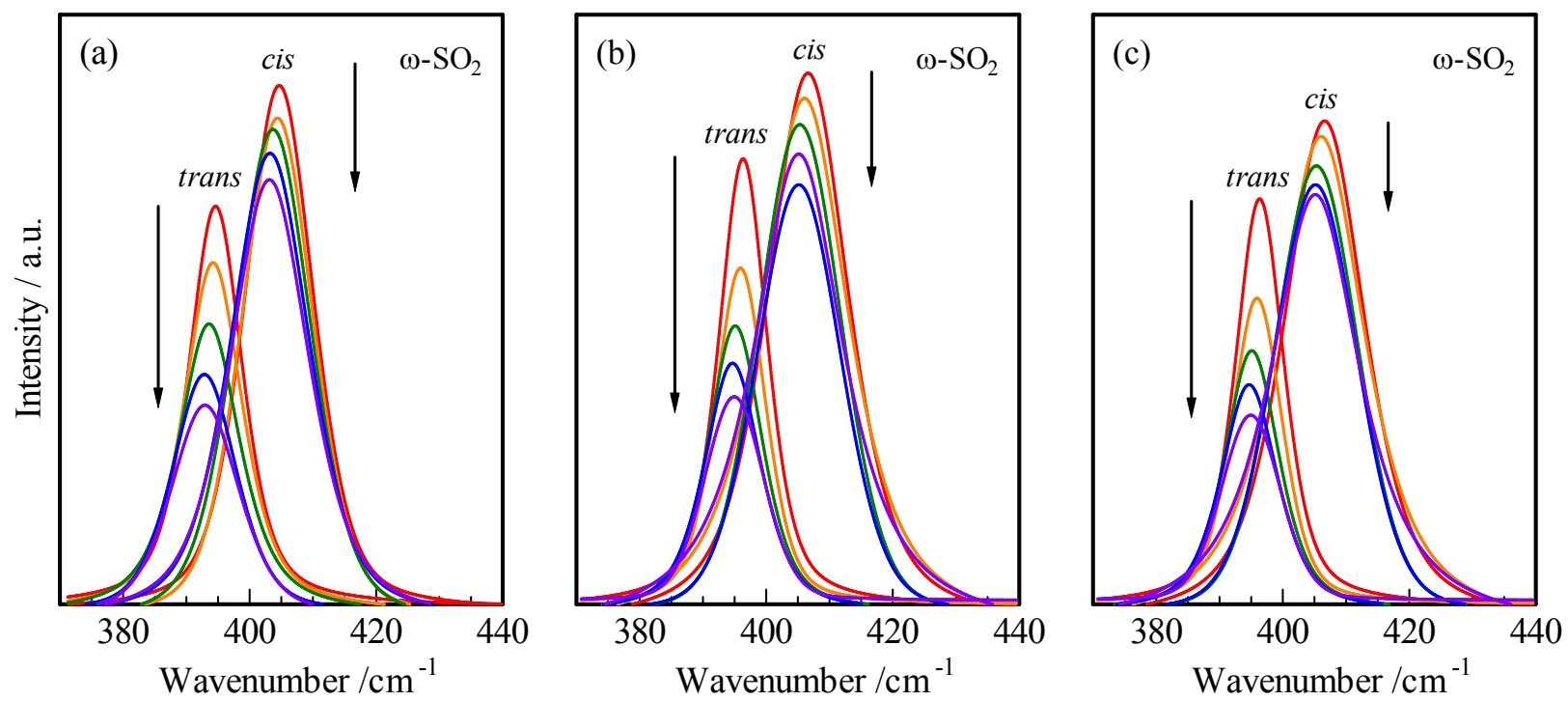●: M^{2+} (M=Fe, Co, Ni), ●:C, ●:N, ●:O, ●:F, ●:S
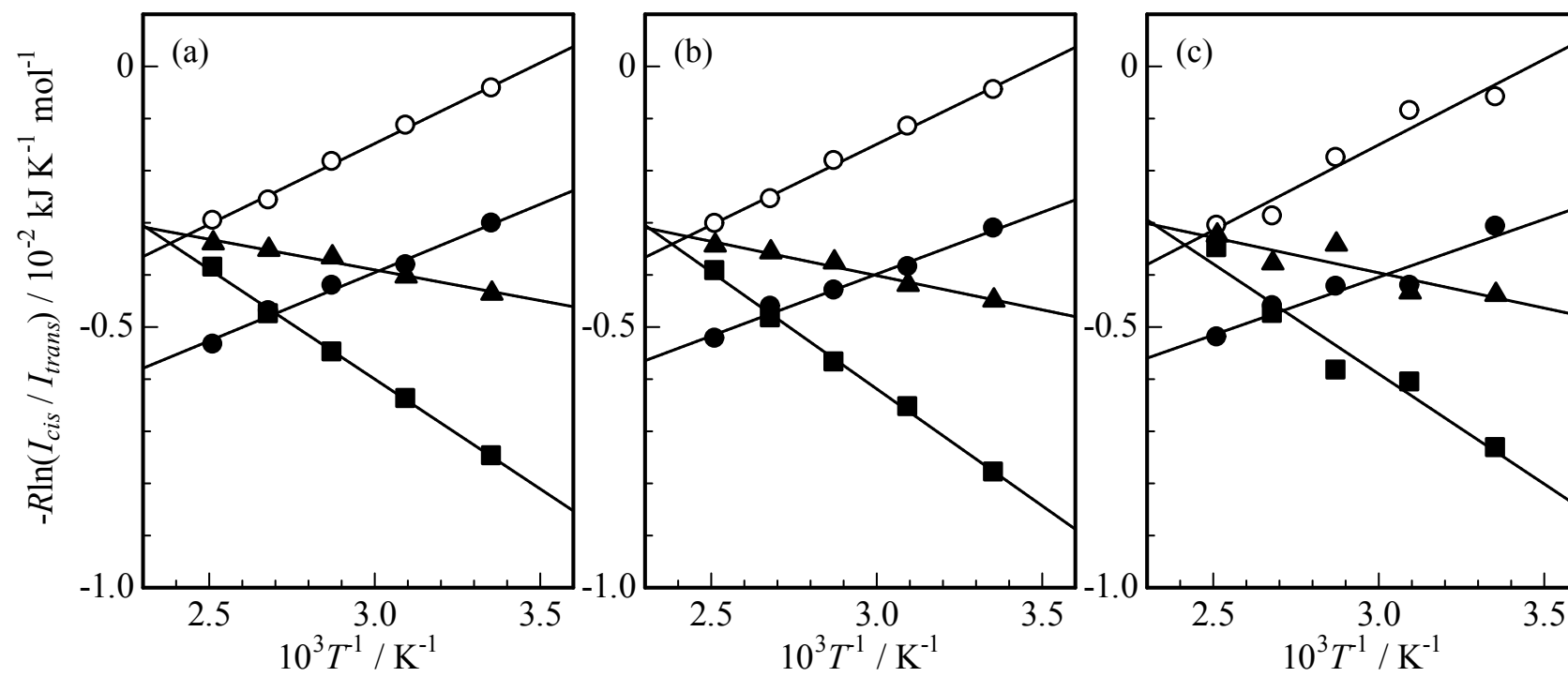
Fig.1

Fig.2
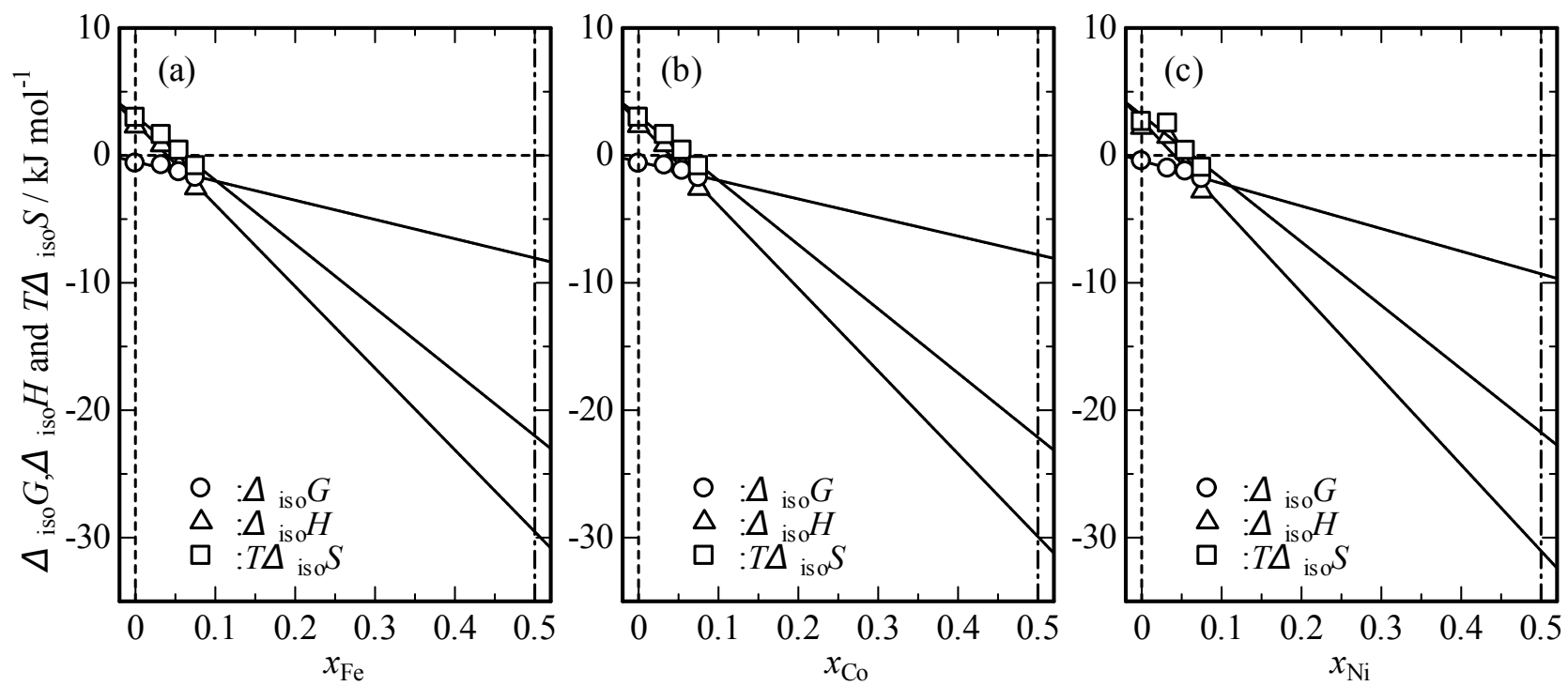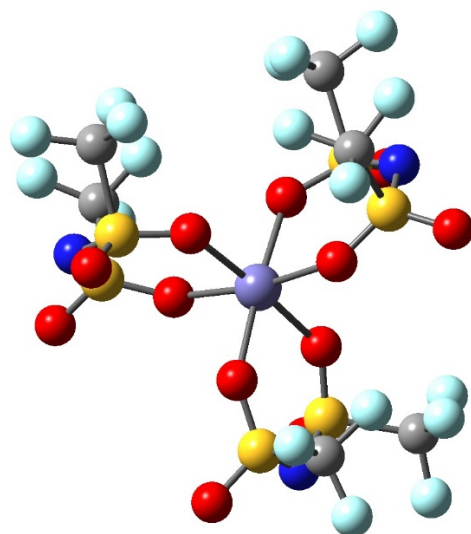
Fig.3

Fig.4

Fig.5

Fig. 6

Table 1 Thermodynamic properties for the isomerism of $[NTf_2]^-$ from the *trans*- to *cis*-isomer in bulk and the first solvation sphere of Fe^{2+}, Co^{2+} and Ni^{2+} in $[P_{2225}][NTf_2]$ at 298 K.

	bulk	first solvation sphere		
		Fe^{2+}	Co^+	Ni^{2+}
$\Delta_{iso}G$ / kJ mol^{-1}	-1.06	-7.53	-7.79	-9.30
$\Delta_{iso}H$ / kJ mol^{-1}	6.86	-29.54	-29.92	-31.04
$T\Delta_{iso}S$ / kJ mol^{-1}	7.92	-22.01	-22.13	-21.75

Table 2 The bond length, the bond angle, the dihedral angle and the dipole moment for the optimized geometries of $[M^{(II)}(cis\text{-}NTf_2)_3]^-$ (M=Fe, Co and Ni) clusters.

Clusters	$[Fe^{(II)}(cis\text{-}NTf_2)_3]^-$	$[Co^{(II)}(cis\text{-}NTf_2)_3]^-$	$[Ni^{(II)}(cis\text{-}NTf_2)_3]^{2-}$
	Bond distance, r / Å		
M^{2+}-O'	2.149	2.163	2.158
N-S	1.613	1.638	1.624
S-O	1.451	1.476	1.483
S-O'	1.482	1.496	1.488
S-C	1.873	1.861	1.890
C-F	1.326	1.348	1.351
	Bond angle, θ / deg.		
M^{2+}-O'-S	135.4	134.9	137.6
O- M^{2+}-O'	83.7	84.1	84.5
S-N-S	125.6	126.2	127.1
N-S-O	112.9	111.8	112.8
N-S-C	103.7	103.1	103.5
O-S-C	103.4	102.6	103.8
O-S-O'	117.5	116.8	118.2
S-C-F	109.8	111.4	111.6
F-C-F	109.4	108.9	109.7
	Dihedral angle, φ / deg.		
S-N-S-C	118.3	119.4	118.9
S-N-S-C	-100.6	-101.3	-101.8
	Dipole moment, μ / D		
	4.07	4.24	4.38